Available online at www.sciencedirect.com
ScienceDirect
Journal of Hazardous Materials 155 (2008) 144–152
Journal of Hazardous Materials
www.elsevier.com/locate/jhazmat

Burning velocity measurements of nitrogen-containing compounds

Kenji Takizawa*, Akifumi Takahashi, Kazuaki Tokuhashi, Shigeo Kondo, Akira Sekiya

National Institute of Advanced Industrial Science and Technology (AIST), Central 5, 1-1-1 Higashi, Tsukuba, Ibaraki 305-8565, Japan

Received 25 January 2007; received in revised form 12 November 2007; accepted 14 November 2007
Available online 18 January 2008

Abstract

Burning velocity measurements of nitrogen-containing compounds, i.e., ammonia (NH_3), methylamine (CH_3NH_2), ethylamine ($C_2H_5NH_2$), and propylamine ($C_3H_7NH_2$), were carried out to assess the flammability of potential natural refrigerants. The spherical-vessel (SV) method was used to measure the burning velocity over a wide range of sample and air concentrations. In addition, flame propagation was directly observed by the schlieren photography method, which showed that the spherical flame model was applicable to flames with a burning velocity higher than approximately 5 cm s^{-1}. For CH_3NH_2, the nozzle burner method was also used to confirm the validity of the results obtained by closed vessel methods. We obtained maximum burning velocities ($S_{u0,max}$) of 7.2, 24.7, 26.9, and 28.3 cm s^{-1} for NH_3, CH_3NH_2, $C_2H_5NH_2$, and $C_3H_7NH_2$, respectively. It was noted that the burning velocities of NH_3 and CH_3NH_2 were as high as those of the typical hydrofluorocarbon refrigerants difluoromethane (HFC-32, $S_{u0,max}$ = 6.7 cm s^{-1}) and 1,1-difluoroethane (HFC-152a, $S_{u0,max}$ = 23.6 cm s^{-1}), respectively. The burning velocities were compared with those of the parent alkanes, and it was found that introducing an NH_2 group into hydrocarbon molecules decreases their burning velocity.
© 2007 Elsevier B.V. All rights reserved.

Keywords: Ammonia; Amine; Spherical vessel; Schlieren photography; Refrigerant

1. Introduction

Hydrofluorocarbons (HFCs) have been developed as alternatives to chlorofluorocarbons (CFCs) because they have no ozone depletion potential (ODP) and lower global warming potential (GWP) than CFCs. Because of their excellent properties, HFCs have been used as refrigerants, foaming agents, and cleaning solvents. However, although they have lower GWP than CFCs owing to their relatively shorter tropospheric lifetime, HFCs have been regulated as greenhouse gases (GHGs) and target compounds for GHG emission reduction in the Kyoto Protocol. Because of this, natural compounds with even lower GWP than HFCs that possess no fluorine atoms have been considered as alternatives to HFCs. These non-fluorinated alternatives include hydrocarbons, CO_2, and nitrogen-containing compounds such as ammonia (NH_3) and small alkyl amines. These alternatives have thermodynamic properties that make them well suited as refrigerants, since they liquefy readily under pressure. In practice, NH_3 has been used as a refrigerant for relatively large refrigerators and icemakers. Small alkyl amines such as methylamine (CH_3NH_2) and ethylamine ($C_2H_5NH_2$) have not been used as refrigerants but have been widely used in industrial fields. Except for CO_2, these non-fluorinated compounds are flammable, so assessment of their flammability is indispensable for predicting their combustion hazards and for ensuring their safe use. To assess the flammability of a compound, several fundamental properties are used, including burning velocity, flammability limits, and heat of combustion. Among these properties, burning velocity may best characterize the potential power of a fire accident. A considerable number of studies have been reported on burning velocities of small alkanes. Published maximum burning velocities for CH_4 and C_3H_8 fall primarily in the range between 35 and 45 cm s^{-1}. In contrast, information on burning velocities of nitrogen-containing compounds has been limited. For NH_3, burning velocity measurements have been reported by several researchers [1–3]. Ronney [1] measured the behavior of an NH_3/air flame in microgravity. Pfahl et al. [2] measured the flame behavior by the schlieren visualization technique with a 400-L closed vessel. Recently, Jabbour and Clodic [3] measured the burning velocity using the

* Corresponding author. Tel.: +81 29 861 9441; fax: +81 29 861 4770.
E-mail address: k.takizawa@aist.go.jp (K. Takizawa).

0304-3894/$ – see front matter © 2007 Elsevier B.V. All rights reserved.
doi:10.1016/j.jhazmat.2007.11.089

vertical tube method. From these measurements by three different methods, the maximum burning velocity for NH_3 ranges between 6.6 and 8.1 cm s^{-1}. Regarding alkyl amines, several reports have presented the physical and chemical data for potential refrigerants, including CH_3NH_2 [4,5] and $C_2H_5NH_2$ [4]. However, there has been no report on burning velocity data. Because primary alkyl amines structurally resemble NH_3 (an alkyl group replaces one hydrogen atom in NH_3), the burning velocities of the amines may be expected to be between those of NH_3 and parent alkanes with an equivalent carbon chain length.

Because of the existence of a C–N bond, CH_3NH_2 has been studied as a model compound for investigating NO_x formation mechanisms. The thermal decomposition of CH_3NH_2/Ar mixtures in shock waves was studied by Dorko et al. [6] over the temperature range $1275 < T < 2400$ K and pressure range $1 < P < 10$ atm. They observed first-order decomposition of CH_3NH_2 and first-order formation of NH_3, with the decomposition rate constant being approximately twice the formation rate constant. According to their results, the predominant initial reaction was C–N bond scission for the decomposition of CH_3NH_2. Gardiner and co-workers measured the time profiles of laser absorption spectra of CH_3NH_2 and obtained its disappearance rate in the reflected shock waves to investigate the reaction mechanisms of thermal decomposition within $1400 < T < 1820$ K [7] and oxidation within $1260 < T < 1600$ K [8]. Kantak et al. [9] investigated modeling of CH_3NH_2 oxidation in a flow reactor at 1160 and 1460 K and compiled experimental kinetic data from several researchers. To our knowledge, however, there are no reported data on the burning velocity of CH_3NH_2.

To understand the flammability of nitrogen-containing compounds and predict the burning velocities of various types of such compounds, the accumulation of burning velocity data is indispensable. For burning velocity measurements, a number of techniques have been developed, such as the burner method, the closed-vessel method, and the vertical tube method, as has been summarized by Andrews and Bradley [10]. In this study we adopted the spherical-vessel (SV) method. The SV method using a closed vessel with central ignition provides the burning velocity data from a measurement of the pressure development during combustion by assuming a spherical flame propagation model. To allow comparison with other techniques, the SV method derives the burning velocity from data collected sufficiently distant from the wall of the reactor. This characteristic helps the obtained data to be minimally influenced by the cooling effect of the reactor and by sample adsorption with the reactor. The latter seems important especially for amines, because a considerable amount of the amines can be adsorbed on the reactor surface, as will be described in the experimental section, and the concentration of the amines on the reactor surface may become higher than the original sample concentration. We have recently reported on burning velocities for typical alkanes and HFCs [11,12] and on those for binary mixtures of fluoroethanes [13] as model refrigerant combustion reactions by applying the SV method. The impartiality of the method enables us to compare quantitatively the data obtained for the nitrogen-containing compounds with those for the alkanes and HFCs.

This article reports on measurements of the burning velocities of NH_3, CH_3NH_2, $C_2H_5NH_2$, and propylamine ($C_3H_7NH_2$) in particular with respect to their magnitude relative to typical alkanes. The effect of the carbon chain length in the molecule on the burning velocity was also examined. Our approach was to carry out experiments applying two independent techniques using closed vessels with central ignition. The burning velocity of NH_3 was measured by the SV method. Since the SV method can be affected by the buoyancy force on a flame that has a low burning velocity and by wrinkles that can appear on the flame surface, we checked the validity of the spherical flame model by direct measurement of the flame propagation with schlieren photography (the SP method). For the amines, there are no burning velocity data to compare to the data obtained by the SV method. Therefore we also attempted burning velocity measurements using a cylindrical burner for CH_3NH_2, which has a vapor pressure (353 kPa at 298 K) sufficiently high so that the burner method is applicable. We compared the data obtained with those of alkanes and HFC-32 and HFC-152a, which are typical refrigerant compounds, to further understand the flammability of potential natural refrigerants. Finally, structural effects on the burning velocity characteristics of nitrogen-containing compounds are discussed.

2. Experimental

Details of the experimental apparatus, sample preparation, and burning velocity measurements by means of the SV method and schlieren photography have been described previously [11]. Briefly, a mixture of air and NH_3, CH_3NH_2, $C_2H_5NH_2$, or $C_3H_7NH_2$, which was prepared using the partial pressure method, was introduced into a spherical vessel with an inside diameter of 180 mm. It should be noted that since the amines are easily adsorbed on the inner wall of the manifolds and the vessel, the filling pressure of the amines gradually decreases to become roughly 95% of the initial filling pressure after 1 h has passed and then the pressure decrease becomes negligible. Therefore, to obtain accurate sample concentrations, the filling pressure for amines was determined 2 h after introducing the amines, and then the appropriate air pressure for the given amine concentration was introduced into the combustion vessel. The sample was fully mixed by a magnetically driven pump (gas flow rate typically 1.5 L min^{-1}) for 10 min. Ignition was accomplished with an electrical spark between electrodes placed at the center of the vessel. The duration of discharge across the gap was 0.5 ms, and the ignition energy was approximately 100–150 mJ. The pressure development was measured with a Kyowa PHS-10KA absolute pressure transducer and recorded with a Yokogawa DL750 analyzing recorder. After combustion, the final products were drawn from the vessel by a vacuum pump and then were passed through water to dissolve the remaining NH_3 and amines. Sample ignition and pressure–time measurements were performed three times for each concentration at initial pressures of about 600, 700, and 800 Torr (1 Torr = 133 Pa). The initial temperature was the ambient temperature, which was measured with a thermocouple (type K).

Schlieren photography was used to observe flame propagation directly. The photography experiments were conducted in a cylindrical vessel (inner diameter, 155 mm; length, 198 mm) with two quartz windows for optical access. Sample preparation, ignition, pressure measurement, and treatment of the final products in the system were the same as for the SV method. A xenon lamp was used as a light source. The schlieren images of the flame were recorded with an NAC Memrecam Ci digital high-speed CCD video camera and saved on a PC. The framing rate of the video camera was 500 Hz, and the pretrigger time was 20 ms.

For the CH_3NH_2 measurement, a conventional cylindrical burner with inner diameter of 9.6 mm was additionally applied. The experimental apparatus and procedure were almost the same as reported previously [14]. First, the burning velocity of methane (CH_4) was measured to test the reproducibility of the results of the previous report [14]. Then the burning velocity of CH_3NH_2 was measured with the burner and with schlieren visualization. Unfortunately, since the viscous CH_3NH_2 adsorbed inside of the mass flow controller, the mass flow controller soon became sticky with amine and did not work correctly. Therefore, we could obtain only three points for near-stoichiometric mixtures for the burning velocity measurement for CH_3NH_2.

Commercially obtained NH_3 (Taiyo Nippon Sanso, 99.999%), CH_3NH_2 (Mitsubishi Gas Chemical, 99%), $C_2H_5NH_2$ (Tokyo Chemical Industry, 99.7%), $C_3H_7NH_2$ (Wako Pure Chemical Industries, 98%), and CH_4 (Takachiho, 99.99%) were used without further purification.

3. Results and discussion

3.1. Burning velocity measurement

Burning velocities were determined from pressure–time data using the technique described in detail in our previous report [11]. Briefly, the spherical vessel was divided into two imaginary regions (b) and (u), as illustrated in Fig. 9 of Ref. [11] and the adiabatic combustion of (b) region and compression of (u) region were considered. The adiabatic expansion occurs and changes the property of the (b) region from (r_{f0}, V_{b0}, T_0, P_0) to (r_f, V_b, T_b, P) based on equilibrium calculation. Here r_f, V_b, T_b, and P denote radius, volume, temperature, and pressure of (b) region, respectively. The value of r_{f0} was decided in order that the mass burned fraction, x, becomes equal to n/N ($n = 0$–N, N was normally 200). The properties x, r_f, V_b, the unburned gas temperature T_u, T_b, and the specific heat ratio γ_u were obtained as a function of P by spline approximation of N relations. Using the measured P–t curve and the calculated P versus each property, each of the parameters x, r_f, V_b, T_u, T_b, and γ_u was obtained as a function of t. Using these parameters the burning velocity S_u for adiabatic combustion in the spherical vessel is expressed by the following equation:

$$S_u = \frac{R}{3}\left[1-(1-x)\left(\frac{P_0}{P}\right)^{1/\gamma_u}\right]^{-2/3}\left(\frac{P_0}{P}\right)^{1/\gamma_u}\frac{dx}{dt}, \quad (1)$$

where R is the inside radius of the vessel.

This technique is based on the assumption that the flame front is smooth and remains spherical during propagation. The spherical flame assumption is considered valid when the burning velocity is greater than about 5 cm s^{-1}. In the SV method, the burning velocity, S_u, was experimentally obtained as a function of temperature (T) and pressure (P) because the unburned region in the closed vessel was compressed adiabatically during flame propagation. Therefore, S_u was fitted to the following empirical equation:

$$S_u = S_{u0}\left(\frac{T}{T_s}\right)^{\alpha}\left(\frac{P}{P_s}\right)^{\beta}. \quad (2)$$

where $T_s = 298$ K, $P_s = 1$ atm, S_{u0} is the burning velocity at T_s and P_s, and α and β are the fitting parameters for the temperature and pressure dependencies, respectively. At each concentration, we took measurements at 600, 700, and 800 Torr of initial pressure (P_0). S_{u0} was obtained by applying Eq. (2) to the results at the three initial pressures. Figs. 1(a), 2(a), and 3 show the measured S_{u0} values as a function of equivalence ratio (ϕ) for NH_3 and the three amines. The calculations of ϕ were based on the following overall reaction:

$$C_nH_{2n+1}NH_2 + \frac{6n+3}{4}O_2 = nCO_2 + \frac{2n+3}{2}H_2O + 0.5N_2 \quad (n = 0\text{–}3). \quad (R1)$$

Since S_{u0}, α, and β depend on ϕ, we performed a nonlinear least-squares fitting of all the data measured at various concentrations using the following equations:

$$S_{u0} = S_{u0,max} + s_1(\phi - \phi_{max})^2 + s_2(\phi - \phi_{max})^3, \quad (3)$$

$$\alpha = a_1 + a_2(\phi - 1), \quad (4)$$

$$\beta = b_1 + b_2(\phi - 1), \quad (5)$$

where $S_{u0,max}$, s_1, s_2, ϕ_{max}, a_1, a_2, b_1, and b_2 are the fitting parameters. $S_{u0,max}$ is the maximum burning velocity at T_s, P_s, and ϕ_{max} and a_1 and b_1 are the values of α and β, respectively, at $\phi = 1$. The cubic form of Eq. (3) represents the asymmetric nature of the ϕ dependence of the burning velocity. In the figures, the filled symbols denote the observed values from the measurements for each concentration, and the curves denote Eq. (3) obtained by the above procedure. From these curves, the maximum burning velocities $S_{u0,max}$ and the corresponding equivalence ratios ϕ_{max} were obtained.

3.2. Burning velocity of NH_3

We first measured the burning velocities for NH_3/air mixtures by the SV method and compared the results with previously reported values. Fig. 1(a) shows the burning velocities of NH_3/air mixtures as a function of ϕ, along with published data obtained by a microgravity experiment [1], measurement of the flame radius in a closed vessel [2], and the vertical tube method [3]. We obtained a value for $S_{u0,max}$ of 7.2 cm s^{-1} at $\phi_{max} = 1.10$. We observed the flame propagation by both

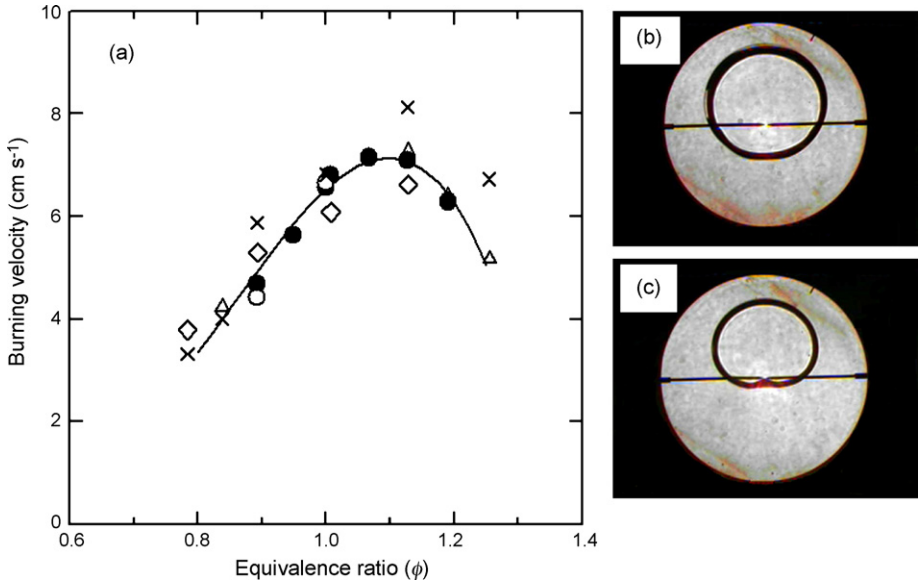

Fig. 1. Burning velocity results of NH_3/air mixtures. (a) Burning velocities as a function of ϕ by the SV method (filled circles and solid curve), the SP method (open circles), closed vessel in microgravity [1] (crosses), closed vessel [2] (diamonds), and vertical tube [3] (triangles). Schlieren images of NH_3/air flames at room temperature and $P_0 = 1.05$ atm for (b) $\phi = 1.0$ (21.9%), $t = 80$ ms and (c) $\phi = 0.89$ (20.0%), $t = 120$ ms.

direct and schlieren photography. In direct photography, a red-colored NH_3/air flame was observed. The emission of the flame was presumably due to the $\tilde{A}^2A_1 \rightarrow \tilde{X}^2B_1$ transition of NH_2. Copeland et al. [15] observed laser-induced fluorescence (LIF) spectra of the $^2A_1 \rightarrow {}^2B_1$ transition of NH_2 in NH_3/O_2 flame at 500–800 nm. Fig. 1(b) and (c) shows schlieren images of the flame for stoichiometric and lean ($\phi = 0.89$) NH_3/air mixtures in the middle stage of flame propagation. The flame of the stoichiometric mixture appeared nearly spherical (Fig. 1(b)), while the flame of the lean mixture was distorted and had a dimple at the bottom (Fig. 1(c)). The flame distortion was caused by a buoyancy force, which increased upward flame propagation.

For a buoyant flame, the burning velocity is obtained by measuring the horizontal growth of the flame front to minimize the effect of buoyancy. Pfahl et al. [2] obtained the burning velocities of NH_3/air mixtures in this manner. In the pre-pressure period of combustion, the burning velocity is approximated by the following expression:

$$S_u = \frac{dr_f}{dt}\frac{\rho_b}{\rho_u} \tag{6}$$

where r_f is the horizontal flame radius measured in the schlieren image, ρ_u is the initial density of unburned gas, and ρ_b is the density of the burned gas obtained from adiabatic equilibrium

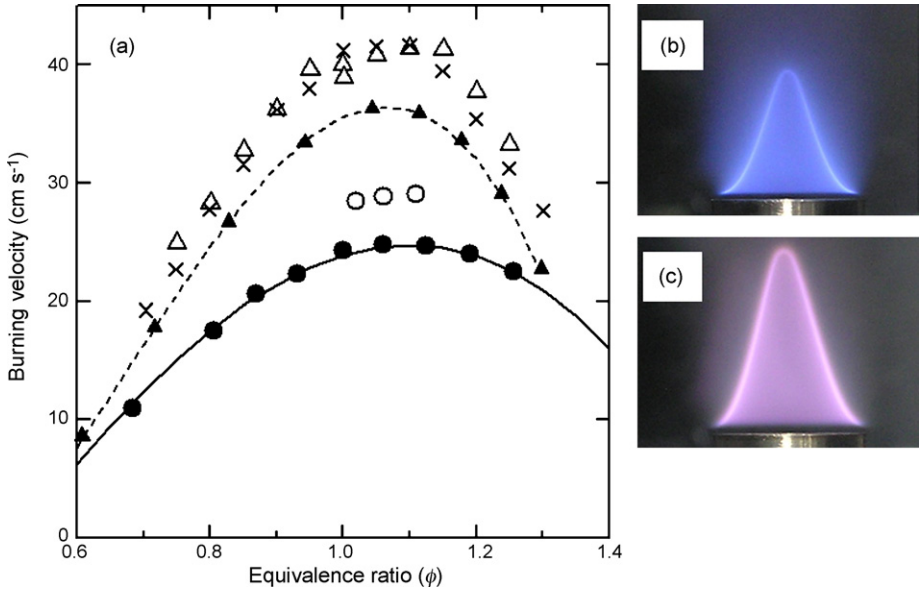

Fig. 2. Burning velocity results of CH_3NH_2/air and CH_4/air mixtures. (a) Burning velocities as a function of ϕ: CH_3NH_2 by the SV method (filled circles and solid curve), CH_3NH_2 by the burner method (open circles), CH_4 by the burner method in this study and in our previous study [14] (open triangles and crosses), and CH_4 by the SV method [11] (triangles and broken curve). Direct color photographs of the burner flames of (b) CH_4/air and (c) CH_3NH_2/air at $\phi = 1.0$.

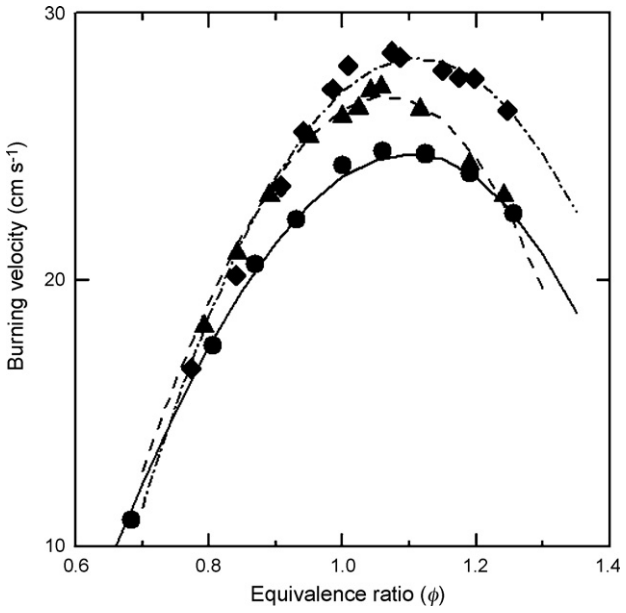

Fig. 3. Burning velocities of alkyl amines/air mixtures as a function of ϕ. CH_3NH_2 (filled circle and solid curve), $C_2H_5NH_2$ (filled triangle and broken curve), and $C_3H_7NH_2$ (filled diamond and dash-dotted curve).

calculation at constant pressure. This approximation is valid as long as the pressure is regarded as constant. In our case, for instance, it took 40 ms to attain 1% increase of the initial pressure for stoichiometric NH_3/air combustion. The corresponding r_f was up to about 1.8 cm. In such a very initial stage of flame propagation, the small flame sphere was affected by the spark and the electrodes. On the other hand, if we apply the data after the pre-pressure period to Eq. (6), the value of dr_f/dt is underestimated because the flame sphere is compressed by its surroundings of increasing pressure. Therefore, we took into consideration the adiabatic compression of the flame as follows. First, we obtained the relationship of r_f and P by performing an equilibrium calculation for a constant volume condition. Then we applied the SV method in the same manner as explained in Appendix of Ref. [11] to the experimental values of r_f to obtain the values of S_{u0}. The burning velocities obtained by the SP method were 6.6 cm s^{-1} at $\phi = 1.0$ and 4.4 cm s^{-1} at $\phi = 0.89$, which are shown as open circles in Fig. 1(a). Compared with published values, the value of $S_{u0,max}$ in the present study was lower by 0.9 cm s^{-1} than that of the microgravity experiment by Ronney [1]. Our value of $S_{u0,max}$ was slightly higher than that of the closed vessel measurement by Pfahl et al. [2]. Our results by the SP method agreed with the results by Pfahl et al.; both methods measured the horizontal flame radii, but the volume of the reactor was different by two orders of magnitude. This difference between the burning velocity measurements may be related to the treatment of the effect of compression of the flame sphere. Our results were close to the values obtained by the vertical tube method [3] for all values of ϕ. In all methods, maximum burning velocities were obtained at $\phi = 1.1$–1.2. These comparisons show that the present NH_3 burning velocity results are quite reasonable.

3.3. Burning velocities of alkyl amines

Fig. 2(a) shows the experimental results of the burning velocity measurements of CH_3NH_2/air mixtures as a function of ϕ. For comparison, the results of CH_4/air mixtures are included in the figure. To analyze comparatively the results of the SV method, we also carried out measurements by using the cylindrical burner method. First, to test the reproducibility of our experiment, we measured the burning velocity of CH_4 by the same system we used in our previous study [14] and compared the results. As shown in the figure, comparison of the results of the present and previous studies shows good reproducibility at all measured concentrations. Second, the results from the burner and SV methods were compared for CH_4/air and CH_3NH_2/air mixtures. Comparison between the results of the SV and burner methods shows that burning velocities measured by the burner method are on average higher by 4.8 and 4.1 cm s^{-1} than those of the SV method for CH_4/air and CH_3NH_2/air mixtures, respectively (Fig. 2(a)). The corresponding percentage errors are 14% for CH_4/air and 13% for CH_3NH_2/air; thus, the measured burning velocities of CH_3NH_2/air mixtures by the two methods have similar errors as those of CH_4/air mixtures. The differences between the results of the SV and burner methods were mainly caused by the flame stretch that appears on the burner edge of a bunsen-type flame. The similar errors between the two methods for CH_4/air and CH_3NH_2/air mixtures suggest that the burning velocities for the amines derived by the SV method are reliable.

Fig. 2(b) and (c) are direct color photographs of the burner flames of stoichiometric CH_4/air and CH_3NH_2/air mixtures, respectively. The flame color of CH_4/air (Fig. 2(b)) may result from the $A^2\Delta \rightarrow X^2\Pi$ transition of CH at a wavelength of 430 nm [16]. To our knowledge, there is no previous report on the spectroscopic measurement of the flame of CH_3NH_2. However, NH_2 radical production was observed by LIF in an infrared multiphoton dissociation study of low pressure CH_3NH_2 by Filseth et al. [17]. They suggested the C–N bond scission, $CH_3NH_2 \rightarrow CH_3 + NH_2$, was one of the most plausible reactions for CH_3NH_2 dissociation. Hwang et al. [8] reported in their shock tube study the significant contribution of a decomposition reaction, $CH_3NH_2 + H \rightarrow CH_3 + NH_3$, in CH_3NH_2 oxidation and calculated the concentrations of NH_3 and NH_2. The color of the observed flame for CH_3NH_2/air (Fig. 2(c)) presumably resulted from the emissions due to the $A \rightarrow X$ transition of CH and the $^2A_1 \rightarrow {}^2B_1$ transition of NH_2. It appears that CH and NH_2 were generated as intermediate species in the CH_3NH_2 combustion process.

Fig. 3 shows the burning velocities for CH_3NH_2/air, $C_2H_5NH_2$/air, and $C_3H_7NH_2$/air mixtures as a function of ϕ. The values of $S_{u0,max}$ were obtained as 24.7, 26.9, and 28.3 cm s^{-1} at $\phi_{max} = 1.10$, 1.07, and 1.11 for CH_3NH_2/air, $C_2H_5NH_2$/air, and $C_3H_7NH_2$/air, respectively. These results indicate that the burning velocity increases as the alkyl group in the amine lengthens. For all amines, maximum burning velocities were obtained at slightly richer concentrations and the values of ϕ_{max} were slightly higher than those of small alkanes [11,12].

To validate the application of the spherical flame model to CH_3NH_2, flame propagation was directly observed using the SP

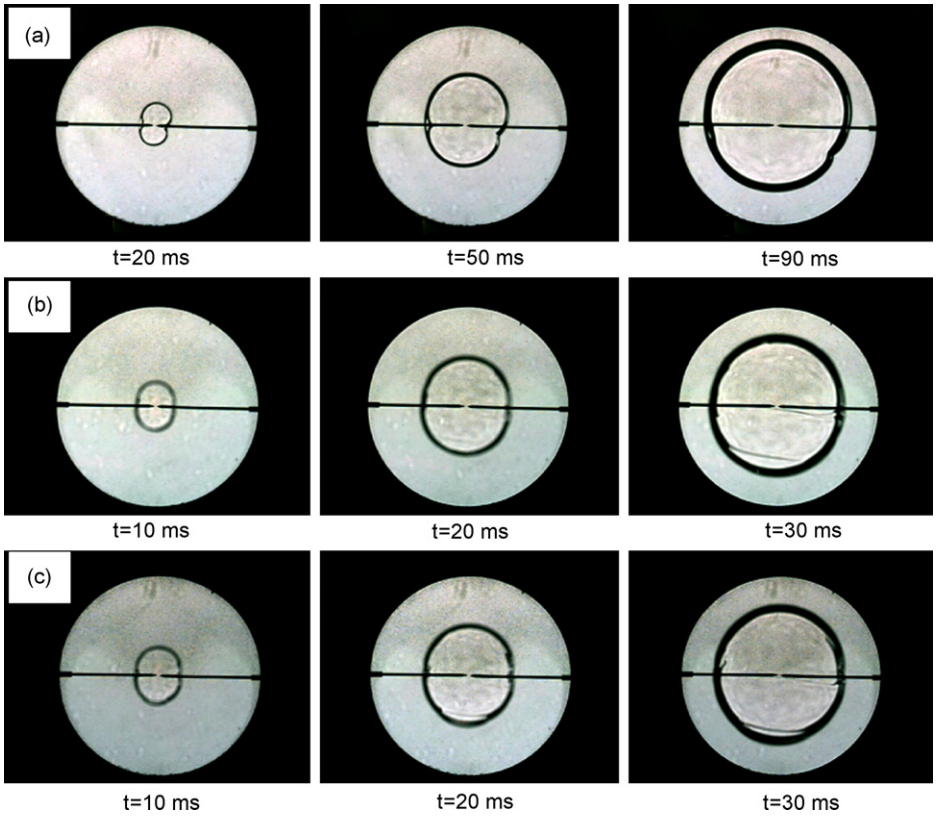

Fig. 4. Schlieren images of the flame propagation for CH_3NH_2/air mixtures at $T_0 = 300$ K, $P_0 = 1$ atm. (a) $\phi = 0.68$ (6.0%), (b) $\phi = 1.0$ (8.54%), (c) $\phi = 1.26$ (10.5%).

method. Fig. 4(a–c) shows time evolutions of schlieren images for flames of the lean, stoichiometric, and rich CH_3NH_2/air mixtures, respectively. In $C_2H_5NH_2$/air and $C_3H_7NH_2$/air flames, quite similar results were observed for the relationship between flame shape and sample equivalence ratio. In these flames, small dimples in the horizontal direction were observed, which were due to a cooling effect of the electrodes. In the figures, the flames propagated almost spherically even in the slowest burning velocity condition ($\phi = 0.68$, S_{u0} about 11 cm s^{-1}), which indicates that the effect of buoyancy was negligibly small. A few wrinkles were observed as the flame propagated outward (Fig. 4(b) and (c)), but such wrinkles were not observed for the lean flame (Fig. 4(a)). If such a discontinuous flame front were to become more developed, a cellular structure would appear, which could increase the flammability. Groff [18] investigated flame propagation for propane/air in various concentrations and initial pressures, in order to observe the onset of cellular structure. In all his experimental conditions, namely, initial pressure in the range of 200–500 kPa, ϕ in the range of 0.7–1.0, and initial temperature near 300 K, the flames should be stable considering the fact that their Lewis numbers are larger than unity. According to his observation, however, all the flames formed cellular

Table 1
Physical and flammability properties for nitrogen-containing compounds, alkanes, and HFCs

Compound	NBP (°C)[a]	$S_{u0,max}$ (cm s^{-1})[a]	ϕ_{max}[a]	H_c (kJ mol^{-1})[a]	T_{ad} (K)[a]	LFL (vol.%)[a]
NH_3	−33	7.2	1.10	317	2465	15.2[d]
CH_3NH_2	−7	24.7	1.10	975	2664	4.8[e]
$C_2H_5NH_2$	17	26.9	1.07	1586	2664	2.8[e]
$C_3H_7NH_2$	48	28.3	1.11	2199	2665	2.0[e]
CH_4	−161	36.5[b]	1.07[b]	802	2604	4.9[d]
C_2H_6	−89	40.9[c]	1.05[c]	1428	2643	3.0[d]
C_3H_8	−42	38.7[b]	1.06[b]	2044	2652	2.0[d]
CH_2F_2 (HFC-32)	−52	6.7[b]	1.08[b]	486	2610	13.5[e]
CH_3CHF_2 (HFC-152a)	−25	23.6[b]	1.09[b]	1073	2603	4.3[d]

[a] NBP, normal boiling point; $S_{u0,max}$ and ϕ_{max}, maximum burning velocity and the corresponding equivalence ratio, respectively; T_{ad}, adiabatic flame temperature; LFL, lower flammability limit.
[b] From Ref. [11].
[c] From Ref. [12].
[d] From Ref. [21a].
[e] From Ref. [21b].

structures. By considering hydrodynamic effects he concluded the cellular structure occurs above a critical Reynolds number, *Re*, of approximately 4000, where *Re* is defined as the burning velocity multiplied by the flame radius divided by the kinematic viscosity. He also showed critical *Re* is positively correlated to the critical expansion ratio. In the present study, from the viscosity coefficients of 10.09 and 9.43×10^{-6} Pa s at 298 K [19], the values of maximum *Re* were approximately 400 and 1500 for NH_3/air and CH_3NH_2/air, respectively. We could not find the viscosity coefficients of $C_2H_5NH_2$ and $C_3H_7NH_2$ in the literature. Viscosity coefficients for hydrocarbons are known to decrease with increasing relative molar mass [20]. By applying the relationship between the viscosity coefficient and the relative molar mass for hydrocarbons to the alkyl amines, the maximum *Re* values for $C_2H_5NH_2$/air and $C_3H_7NH_2$/air mixtures were estimated to be approximately 1600 and 1700, respectively. These results imply that the flames of these three amines mixed with air do not have a cellular structure. From the direct observation of flames and the estimated values of *Re*, we conclude that the effect of flame wrinkling was not significant in the present experiment. Furthermore, the burning velocities obtained from each concentration (filled symbols in Figs. 2(a) and 3) did not deviate from those obtained from all the concentrations (curves in Figs. 2(a) and 3), which indicates that the obtained burning velocities were valid throughout the entire range of experimental concentrations of the amines without any noticeable increase in the burning velocity caused by flame discontinuity. Therefore, application of the SV method is valid for measuring the burning velocities of these amines.

3.4. Comparison of flammability properties

Table 1 lists the obtained maximum burning velocities for NH_3 and the three amines along with those of alkanes and HFCs [11,12], for comparison. The normal boiling point (NBP), heat of combustion (H_c), adiabatic flame temperature (T_{ad}), and lower flammability limit (LFL) [21] are also listed in the table. The T_{ad} values are the results of an adiabatic equilibrium calculation in a constant volume at $T_0 = 298$ K and $P_0 = 1$ atm. The data show that the amines have higher values of $S_{u0,max}$, H_c, and T_{ad} than NH_3. When compared with HFCs, NH_3 shows similarity to HFC-32 in all the properties listed. CH_3NH_2 and HFC-152a also show similar values for these properties. In addition, the burning velocity for the alkyl amines is considerably lower than that of alkanes, despite the higher values of T_{ad}.

One of the purposes of this study was to ascertain how various structural factors affect the burning velocity of nitrogen-containing compounds. In considering the structural effects, we focused on the primary reactions of combustion, bond dissociation energy, and flame temperature of the amines. The contributions of these factors were considered in the following discussion.

There are no published data on the CH_3NH_2 oxidation mechanism in a constant volume vessel that are directly comparable with the present study. For the reaction rate of CH_3NH_2 oxidation in a flow tube reactor [9], the following important elementary reactions in CH_3NH_2 consumption are shown in order of decreasing integral average rate:

$$CH_3NH_2 + OH = CH_2NH_2 + H_2O \quad (R2)$$

$$CH_3NH_2 + O = CH_2NH_2 + OH \quad (R3)$$

$$CH_3NH_2 + OH = CH_3NH + H_2O \quad (R4)$$

$$CH_3NH_2 + H = CH_3 + NH_3 \quad (R5)$$

$$CH_3NH_2 + O = CH_3NH + OH \quad (R6)$$

$$CH_3NH_2(+M) = CH_3 + NH_2(+M) \quad (R7)$$

The reactions (R2)–(R4) and (R6) are hydrogen abstraction reactions from a CH_3NH_2 molecule. H-atom abstraction occurs nearly equivalently at C-atom and N-atom centers. The reactions (R5) and (R7) are C–N bond scission reactions. Comparison of the results between 1160 and 1460 K at a flow pressure of 0.01 atm [9] shows that among the six reactions, the contribution of C–N bond scission by (R5) and (R7) relatively increased with temperature rise, and that the ratio of C–N bond scission to H-abstraction was 11/89 at 1160 K and increased to 20/80 at 1460 K. In our case, where the flame temperature was much higher than 1460 K, the relative importance of C–N bond scission as expressed by (R5) and (R7) should increase.

If C–N bond scission and subsequent NH_3 and NH_2 production play important roles during our combustion process, the low burning velocity of CH_3NH_2 can be explained by dilution and inhibition effects by the produced NH_3 and NH_2. The produced CH_3 will oxidize through well-known reaction paths of CH_4 and C_2H_6 combustion, while the produced NH_3 and its fragments oxidize through less-reactive NH_3 combustion (dilution effect). The produced H and OH, which are typical active chain carriers in the combustion reaction, will be consumed not only by hydrocarbon species but also by less-reactive NH_3 and its fragments (inhibition effect). For $C_2H_5NH_2$ and $C_3H_7NH_2$, with lower N/C ratios than that of CH_3NH_2, the contribution of NH_3 and NH_2 to the total amine oxidation will become relatively small. Taking this supposition into consideration, we compared concentrations of the active species O, H, and OH in the flame between the nitrogen-containing compounds and the parent alkanes to analyze the effect of the active species on the burning velocity. Fig. 5 shows the calculated mole fractions of the active species and NO in an adiabatic flame under constant volume at $\phi = 1.0$, $T_0 = 298$ K, and $P_0 = 1$ atm as a function of carbon chain length. Comparing the concentrations among the seven compounds shows that the NH_3 flame, which does not contain carbons, has relatively low concentrations of O, H, and OH. Among the other six flames, the concentrations of the active species and NO are nearly constant, although the mole fractions of H and OH for the CH_3NH_2 flame show slightly higher values than those of the other amines and alkanes. This analysis suggests that the equivalence of the concentrations of active species among the three amines and three alkanes is consistent with the dilution and inhibition effects, and as a consequence, the lower burning velocities for the amines and the dependence of carbon chain length on the burning velocity.

On the other hand, we also considered the case that the H-atom abstraction reaction, which appears in the reactions

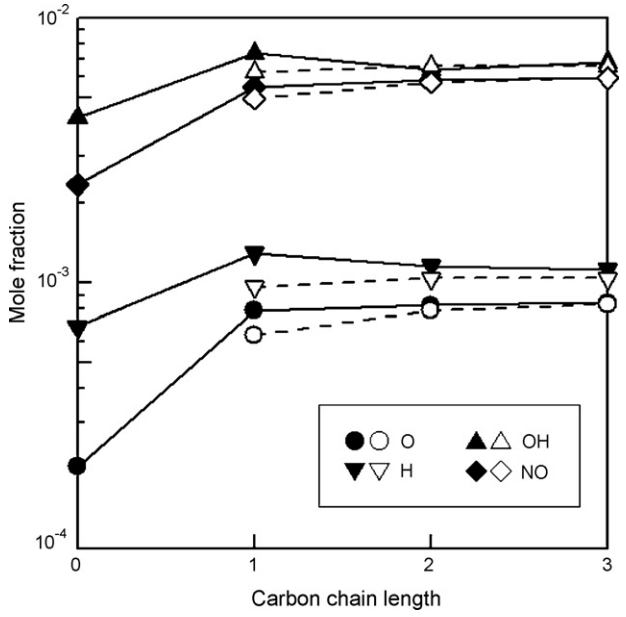

Fig. 5. Effect of the carbon chain length on the mole fractions of chemical species: results for $C_xH_{2x+1}NH_2$ (filled symbols) and C_xH_{2x+2} (open symbols).

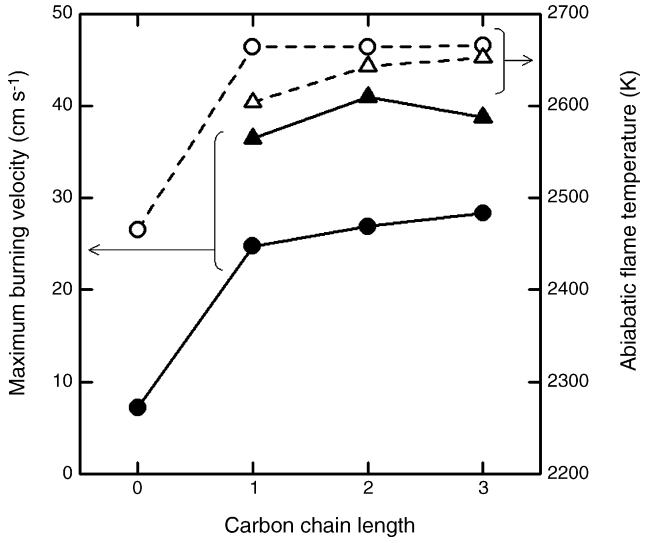

Fig. 6. Effect of the carbon chain length on the maximum burning velocity and flame temperature: $S_{u0,max}$ of $C_xH_{2x+1}NH_2$ and C_xH_{2x+2} (filled circles and filled triangles), T_{ad} of $C_xH_{2x+1}NH_2$ and C_xH_{2x+2} (open circles and open triangles).

(R2)–(R4) and (R6) for CH_3NH_2, was predominant in our combustion process. If the rate of the combustion reaction is determined by H-atom abstraction reactions, then the overall activation energy of combustion is related to the activation energy of H-atom abstraction reactions. An empirical relationship between activation energy and enthalpy of a reaction (Evans–Polanyi rule [22]) has been tested for reactions of OH + alkanes at around room temperature [23]. If the Evans–Polanyi correlation for the reaction of alkanes is also applicable to the reactions of OH + alkyl amines ((R2) and (R4) for CH_3NH_2) and O + alkyl amines ((R3) and (R6) for CH_3NH_2) at high temperatures, then the activation energy is linearly dependent on the magnitude of the bond dissociation energy of C–H (BDE(C–H)) or N–H (BDE(N–H)). Since the N–H bond is stronger than the C–H bond (431 kJ mol^{-1} of BDE(N–H) and 388 kJ mol^{-1} of BDE(C–H) for CH_3NH_2), we compared BDE(C–H) for amines with that for alkanes. The calculated BDE(C–H) values of CH_3NH_2 and $CH_3C^*H_2NH_2$ are 388 and 384 kJ mol^{-1} [24], while the experimental BDE(C–H) values of CH_4, C_2H_6, and $CH_3C^*H_2CH_3$ are 439, 423, and 413 kJ mol^{-1}, respectively [25]. The experimental BDE(N–H) of NH_3 is 453 kJ mol^{-1} [25], slightly higher than BDE(C–H) of CH_4. The lower BDE(C–H) and the subsequent radical stabilization for the amines may be caused by strong electron donating of NH_2 owing to a lone pair of N [24]. From this comparison, we see that H-atom abstraction for amines is more likely to occur than for alkanes. On the basis of the Evans–Polanyi rule, the activation energy of amine oxidation with lower BDE(C–H) is expected to have a lower value than that of alkanes. Considering that amines have lower values of $S_{u0,max}$ than alkanes, H-atom abstraction does not seem to be predominant in the present combustion. The lower BDE(C–N) (354 kJ mol^{-1} for CH_3NH_2 and 340 kJ mol^{-1} for $C_2H_5NH_2$) may also support the preference of C–N bond scission to H-atom abstraction.

Regarding the flame temperature, Fig. 6 shows the measured maximum burning velocity and the calculated adiabatic flame temperature as functions of the carbon chain length. The results of small alkanes are also shown in the figure. NH_3, with an approximately 200 K lower flame temperature than the amines, also shows a lower value of $S_{u0,max}$. For the three alkyl amines, the value of T_{ad} is unchanged by the carbon chain length, while the value of $S_{u0,max}$ increases with increasing carbon chain length. The T_{ad} values of the amines are higher than those of the parent alkanes, even though the three amines have lower $S_{u0,max}$ values than the parent alkanes.

From the above considerations of the primary reactions of amine consumption, BDE, and the adiabatic flame temperature, we conclude that the contribution of the NH_3 and NH_2 production reactions (R5) and (R7) characteristic of primary alkyl amines might reasonably explain why the burning velocities of the amines are lower than those of the parent alkanes. If considerable amounts of NH_3 and NH_2 were produced as intermediates, the produced NH_x as well as CH_x would react with the active chain carriers (O, H, and OH). By these dilution and inhibition effects, the burning velocity would decrease as the concentration of the amino groups increases, even if the amines have higher flame temperature and weaker BDE(C–H) than the parent alkanes. The dependence of $S_{u0,max}$ on carbon chain length and the weaker BDE(C–H) of amines than that of alkanes could also be explained by C–N bond scission and subsequent NH_3 and NH_2 production. As mentioned above, published data on oxidation of amines are so far limited to those at the temperature much lower than our case. To make clear the detailed combustion mechanism, quantitative analysis of chemical species in the flame and construction of a detailed chemical reaction model will be necessary. For further understanding it would also be interesting to investigate the flammability of dimethylamine or trimethylamine, since they may initially decompose to produce NH or N but not NH_3 or NH_2.

4. Conclusion

Burning velocities were obtained for NH_3 and C_1–C_3 primary alkyl amines by employing the spherical-vessel method. The validity of the obtained data was tested by the schlieren photography method, and for CH_3NH_2 the burner method was also applied. Comparison of fundamental properties with HFCs and alkanes showed that NH_3 and CH_3NH_2 resemble the flammability properties of the typical refrigerants CH_2F_2 and CH_3CHF_2, respectively, including the maximum burning velocity. The amines showed lower burning velocities than the parent alkanes despite the lower C–H bond dissociation energy and higher flame temperature, which may be because C–N bond scission and subsequent NH_3 and NH_2 production reactions play important roles in the combustion reaction of alkyl amines.

Acknowledgement

This work was partially supported by the New Energy and Industrial Technology Development Organization (NEDO) within the framework of new energy, energy conservation, and environment-related projects.

References

[1] P.D. Ronney, Effect of chemistry and transport properties on near-limit flames at microgravity, Combust. Sci. Technol. 59 (1988) 123–141.
[2] U.J. Pfahl, M.C. Ross, J.E. Shepherd, K.O. Pasamehmetoglu, C. Unal, Flammability limits, ignition energy, and flame speeds in H_2–CH_4–NH_3–N_2O–O_2–N_2 mixtures, Combust. Flame 123 (2000) 140–158.
[3] T. Jabbour, D. Clodic, Burning velocity and refrigerant flammability classification, ASHRAE Trans. 110 (2004) 522–533.
[4] J.M. Calm, G.C. Hourahan, Refrigerant data summary, Eng. Syst. 18 (November (11)) (2001) 74–88.
[5] J. Jones, Nearly azeotropic mixtures to replace refrigerant 12, NASA Tech Brief 16 (8) (1992).
[6] E.A. Dorko, N.R. Pchelkin, J.C. Wert III, G.W. Mueller, Initial shock tube studies of monomethylamine, J. Phys. Chem. 83 (1979) 297–302.
[7] T. Higashihara, W.C. Gardiner Jr., S.M. Hwang, Shock tube and modeling study of methylamine thermal decomposition, J. Phys. Chem. 91 (1987) 1900–1905.
[8] S.M. Hwang, T. Higashihara, K.S. Shin, W.C. Gardiner Jr., Shock tube modeling study of monomethylamine oxidation, J. Phys. Chem. 94 (1990) 2883–2889.
[9] M.V. Kantak, K.S. de Manrique, R.H. Aglave, R.P. Hesketh, Methylamine oxidation in a flow tube reactor: mechanism and modeling, Combust. Flame 108 (1997) 235–265.
[10] G.E. Andrews, D. Bradley, Determination of burning velocities: a critical review, Combust. Flame 18 (1972) 133–153.
[11] K. Takizawa, A. Takahashi, K. Tokuhashi, S. Kondo, A. Sekiya, Burning velocity measurement of fluorinated compounds by spherical-vessel method, Combust. Flame 141 (2005) 298–307.
[12] K. Takizawa, A. Takahashi, K. Tokuhashi, S. Kondo, A. Sekiya, Burning velocity measurement of HFC-41, HFC-152, and HFC-161 by the spherical-vessel method, J. Fluorine Chem. 127 (2006) 15470–21553.
[13] K. Takizawa, A. Takahashi, K. Tokuhashi, S. Kondo, A. Sekiya, Reaction stoichiometry for combustion of fluoroethane blends, ASHRAE Trans. 112 (2006) 459–468.
[14] K. Tokuhashi, Y. Urano, S. Horiguchi, S. Kondo, Incineration of CFC-12 by burner methods, Combust. Sci. Technol. 72 (1990) 117–129.
[15] R.A. Copeland, D.R. Crosley, G.P. Smith, Laser-induced fluorescence spectroscopy of NCO and NH_2 in atmospheric pressure flames, in: Twentieth Symposium (International) on Combustion, The Combustion Institute, Pittsburgh, 1984, pp. 1195–1203.
[16] D.E. Heard, J.B. Jeffries, G.P. Smith, D.R. Crosley, LIF measurements in methane/air flames of radicals important in prompt-no formation, Combust. Flame 88 (1992) 137–148.
[17] S.V. Filseth, J. Danon, D. Feldmann, J.D. Campbell, K.H. Welge, Infrared multiple-photon dissociation of N_2H_4 and CH_3NH_2. Fluence dependence of the production of NH_2, Chem. Phys. Lett. 63 (1979) 615–620.
[18] E.G. Groff, The cellular nature of confined spherical propane–air flames, Combust. Flame 48 (1982) 51–62.
[19] L.G. Burch, C.J.G. Raw, Transport properties of polar-gas mixtures. I. Viscosities of ammonia-methylamine mixtures, J. Chem. Phys. 47 (1967) 2798–2801.
[20] D.L. Katz, D. Cornell, R. Kobayashi, F.H. Poetmann, J.A. Vary, J.R. Elenblass, C.F. Weinaug, Handbook of Natural Gas Engineering, McGraw-Hill, New York, 1959.
[21] (a) S. Kondo, K. Takizawa, A. Takahashi, K. Tokuhashi, Extended Le Chatelier's formula and nitrogen dilution effect on the flammability limits, Fire Safety J. 41 (2006) 406417;
(b) S. Kondo, Private results measured by the same method of Ref. [21(a)].
[22] M.G. Evans, M. Polanyi, Inertia and driving force of chemical reactions, Trans. Faraday Soc. 34 (1938) 11–29.
[23] N. Cohen, Are reaction rate coefficients additive? Revised transition state theory calculations for OH + alkane reactions, Int. J. Chem. Kinet. 23 (1991) 397–417.
[24] D.D.M. Wayner, K.B. Clark, A. Rauk, D. Yu, D.A. Armstrong, C–H bond dissociation energies of alkyl amines: radical structures and stabilization energies, J. Am. Chem. Soc. 119 (1997) 8925–8932.
[25] J. Berkowitz, G.B. Ellison, D. Gutman, Three methods to measure RH bond energies, J. Phys. Chem. 98 (1994) 2744–2765.